

Integrin and matrix metalloprotease dual-targeting with an MMP substrate–RGD conjugate†

Cite this: *Org. Biomol. Chem.*, 2013, **11**, 448Christiane H. F. Wenk,^{a,b,c} Véronique Josserand,^{b,c} Pascal Dumy,^{a,c} Jean-Luc Coll^{*b,c} and Didier Boturyn^{*a,c}Received 1st October 2012,
Accepted 14th November 2012

DOI: 10.1039/c2ob26926k

www.rsc.org/obc

A fluorescent clustered RGD-containing ligand encompassing an MMP substrate was designed and successfully used *in vivo* for the dual-targeting of $\alpha_v\beta_3$ integrin receptors and MMP-9 extracellular proteases in the tumor region.

Introduction

The identification of molecular markers that can differentiate a tumor from healthy tissue represents a major goal in cancer medicine. In this context, integrins, such as $\alpha_v\beta_3$, are attractive therapeutic targets.¹ These receptors are cell surface proteins that are highly expressed on tumor blood vessels during angiogenesis and on various tumor cells. A characteristic feature of the $\alpha_v\beta_3$ integrin is its high binding affinity for the ubiquitous triad sequence arginine-glycine-aspartic acid (RGD) of proteins such as vitronectin, fibronectin, osteopontin, which belong to the extracellular matrix. The design of numerous RGD-containing cyclopeptides has led to highly selective synthetic ligands with enhanced binding affinities.² Such peptides were further exploited for drug delivery and tumor imaging.³ For instance, *in vivo* targeting of tumor vasculature using RGD conjugates opens up new perspectives for cancer detection and management^{4,5} including imaging-guided surgery.⁶

We have shown that a clustered RGD-containing compound bearing a cytotoxic peptide offers an interesting outlook for tumor-targeted drug delivery.⁷ Enzymatic reduction of a disulfide bond was used for the drug release within intracellular compartments.⁸ To enhance the tumor selectivity, we describe in this report a dual targeting strategy exploiting the over-expression of $\alpha_v\beta_3$ integrin and active matrix metalloproteases (MMPs) in neovasculature that could be used for the drug delivery instead of enzymatic reduction of a disulfide bridge. Very recently, MMP was used for the activation of cell

penetrating peptide-bearing dendrimers for the *in vivo* fluorescence and magnetic resonance imaging (MRI) of proteases.⁹ We then designed the peptidic macromolecule **1** (Fig. 1) comprising integrin-binding RGD motifs and an MMP-9 cleavable sequence as MMP-9 over-expression has been shown to be involved in cancer angiogenesis¹⁰ and tumor cell invasion.¹¹ An imaging function was used to monitor the MMP activity. We decided to exploit an activatable fluorescent system based on the self-quenching of cyanine 5 fluorescent dyes.¹² A cyclodecapeptide scaffold allows a spatial separation between the targeting and the drug-delivery domains such that the individual properties of both motifs are not affected. With the molecule in hand, we focused our work on assessing biological activities to determine the potency of the MMP-activatable RGD-containing macromolecule.

Results and discussion

Chemical synthesis and characterization of fluorescent conjugate

The synthesis of activatable fluorescent conjugate **1** is reported in Scheme 1. Stable oxime bonds were utilized to append aldehyde-bearing RGD motifs to the cyclodecapeptide scaffold before grafting the MMP-9 peptidic sequence. All peptides were prepared *via* solid-phase peptide syntheses (SPPS) according to methods already developed by our group.¹³ Aminoxy groups were directly incorporated during the SPPS by using 1-ethoxyethylidene containing building blocks.¹⁴ The following head-to-tail cyclisation provided the fully protected cyclodecapeptide **4**. Full deprotection of peptide **4** under acidic conditions allowed the grafting of glyoxylyl aldehyde containing RGD targeting elements (Scheme 1). The subsequent oxidative cleavage with sodium periodate of the amino-alcohol moiety of serine furnished the peptide intermediate **5** in satisfying 66% overall yield.

^aDépartement de Chimie Moléculaire, CNRS: UMR 5250, ICMG FR 2607, Grenoble cedex 9, France. E-mail: didier.boturyn@ujf-grenoble.fr

^bINSERM U823, Grenoble, France. E-mail: jean-luc.coll@ujf-grenoble.fr; Fax: +33 4 7654 9413; Tel: +33 4 7654 9553

^cUniversité Joseph Fourier – Grenoble I, 570, rue de la chimie, BP53, 38041 Grenoble cedex 9, France. Fax: +33 4 5652 0803; Tel: +33 4 5652 0832

†Electronic supplementary information (ESI) available: Synthesis, RP-HPLC profile and ESI-MS of compounds **1**, **4**–**6**; fluospectroscopy, flow cytometry analysis and *in vivo* fluorescence imaging procedures. See DOI: 10.1039/c2ob26926k

Chemoselective addition of MMP peptide **6** on scaffold **5** was carried out in aqueous solution to obtain the peptide conjugate in 46% yield after purification. As expected,¹³

transoximation reaction did not occur during the second oxime ligation. Finally, the use of activated ester of cyanine 5 afforded activatable fluorescent conjugate **1**. Compound **1** was readily purified by reversed-phase HPLC methods and obtained in 31% yield. It was then characterized by electro-spray ionization mass spectrometry (see the ESI†).

The fluorescence emission properties of compound **1** were then evaluated *in vitro*. When the cyanine 5 moieties are linked through the MMP sequence, an intramolecular quenching of Cy5 was observed at 665 nm (Φ/Φ (Cy5) \sim 30%) as was previously observed for other linkers.^{12,15} Treatment with active MMP-9 protease resulted in the expected recovery of the fluorescence intensity (Fig. 2). The spectrum after MMP cleavage matches that of control cyanine 5-containing peptide **7** prepared as described.¹⁶ It is worth noting that compound **1** was found to be stable in buffer and plasma (see the ESI†). In parallel, the MMP-9 activity was carefully monitored by RP-HPLC (Fig. 3). Peptide fragment **2** was characterized by electrospray ionization mass spectrometry without ambiguity since we found the deconvoluted mass to be in total agreement with the calculated mass ($M_{\text{calc}} = 5171.39$, $M_{\text{found}} = 5171.4$).

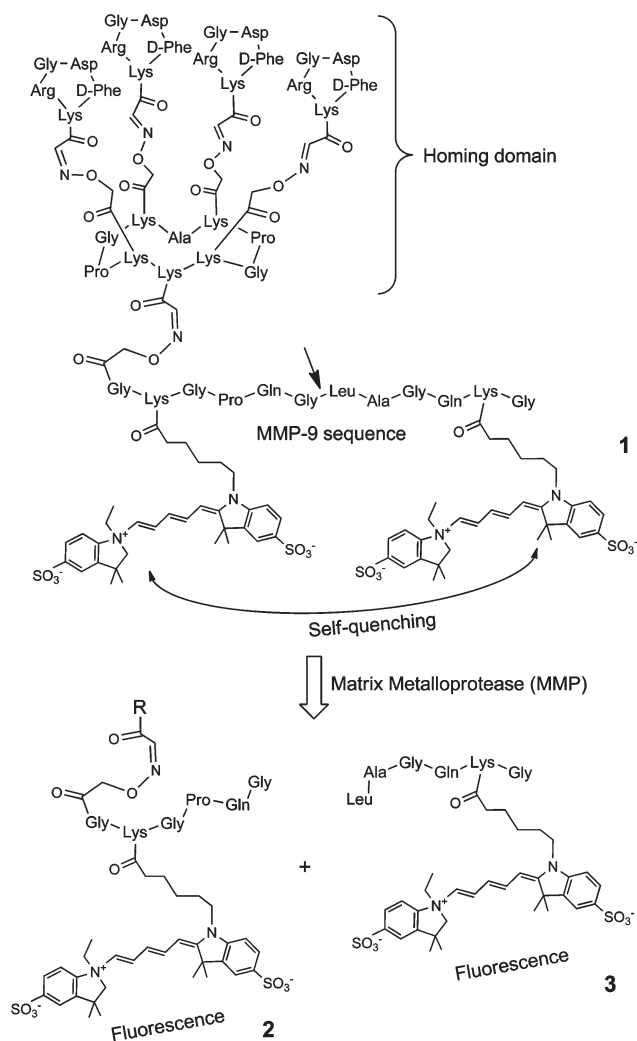


Fig. 1 Chemical structure of activatable fluorescent conjugate **1** (R = homing domain) bearing RGD ligands and MMP-9 cleavable sequence (the arrow shows the MMP-9 cleavage site).

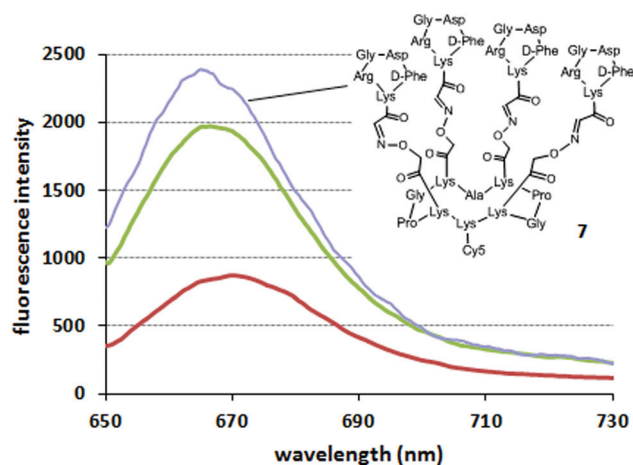
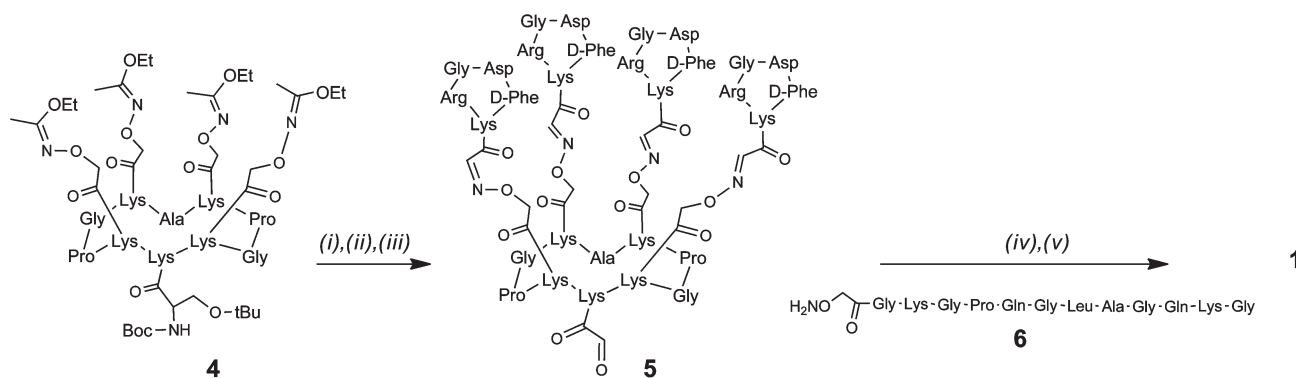


Fig. 2 Emission spectra for compound **1** (red), after addition of MMP-9 (green) at 24 h, and for control Cy5-containing peptide **7** (blue).



Scheme 1 Synthesis of **1**. (i) TFA-TIS-H₂O (95 : 2.5 : 2.5); (ii) 8.5 equiv. cyclo[Arg-Gly-Asp-D-Phe-Lys(CO-CHO)], H₂O; (iii) 10 equiv. NaIO₄, H₂O; (iv) 1.1 equiv. **6**, H₂O-CH₃CN (1 : 1); 2.6 equiv. Cy5-OSu, DMF, DIEA (pH 8.0).

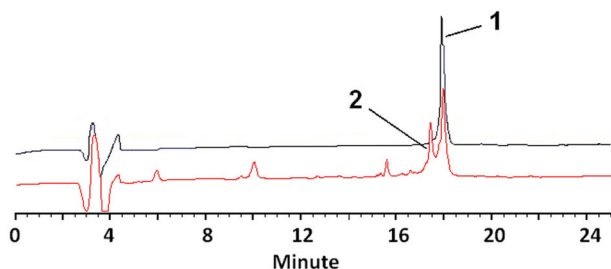


Fig. 3 HPLC profiles (214 nm) for compound **1** (black line) and after treatment with active MMP-9 protease (red line).

In vivo biological studies

We examined the behavior of compound **1** when injected into tumor-bearing mice. Several cell lines that differ in the expression of $\alpha_v\beta_3$ integrin and MMP-9 were selected. We decided to exploit the strongly $\alpha_v\beta_3$ -positive HEK293(β_3) human embryonic kidney cells, $\alpha_v\beta_3$ -positive TS/A-pc mouse mammary carcinoma cells and A375 human melanoma cells, and $\alpha_v\beta_3$ -negative HT1080 human fibrosarcoma cells. Integrin expression was monitored by flow cytometry using $\alpha_v\beta_3$ antibody (see the ESI†).

We then analyzed the capacity of activatable fluorescent compound **1** for the dual targeting of $\alpha_v\beta_3$ integrin and MMP-9. Nude mice bearing subcutaneous tumor xenografts received an intravenous injection of 2 nmol of **1**. To enable the MMP activity and the integrin expression, control mice were injected respectively with 2 nmol of commercially available MMPsense 680¹⁷ or 2 nmol of fluorescent control peptide **7**. It is important to note that we routinely used a higher concentration of peptide **7** (10 nmol) for an optimal tumor imaging.¹⁸ To establish the benefit of MMP, we decided to decrease the amount of the injected compound. Nude mice bearing tumor xenografts were then imaged at 24 h. As shown in Fig. 4, we found significantly lower MMP-9 activity in TS/A-pc than in other tumors. As expected, we observed a similar tumor uptake of cyanine 5-containing peptide **7** for control mice except for nude mice bearing tumor xenografts of HT1080. This result is in agreement with observed $\alpha_v\beta_3$ integrin expression by means of flow cytometry. When mice received activatable fluorescent compound **1**, a strong fluorescence signal showing the dequenching efficiency from MMP-9 was observed for mice bearing HEK(β_3) while low emission was found in HT1080 tumor (dark grey bar, Fig. 4). These findings suggest that $\alpha_v\beta_3$ integrin expression is mandatory for the binding of compound **1** prior to the subsequent proteolytic cleavage from MMP-9, as HT1080 is a cell line known to highly express MMP-9.¹⁹ Interestingly, more fluorescence was found in the TS/A-pc tumor than in the HT1080. This result confirms that activatable peptide **1** accumulates within the $\alpha_v\beta_3$ -containing tumor, at best, as efficiently as control peptide **7**, then preventing its blood clearance. For tumors that expressed both $\alpha_v\beta_3$ integrin and MMP-9 (HEK- β_3 and A375 tumors), the fluorescence signal is proportional to the observed integrin expression. Altogether, this study clearly shows the interest of

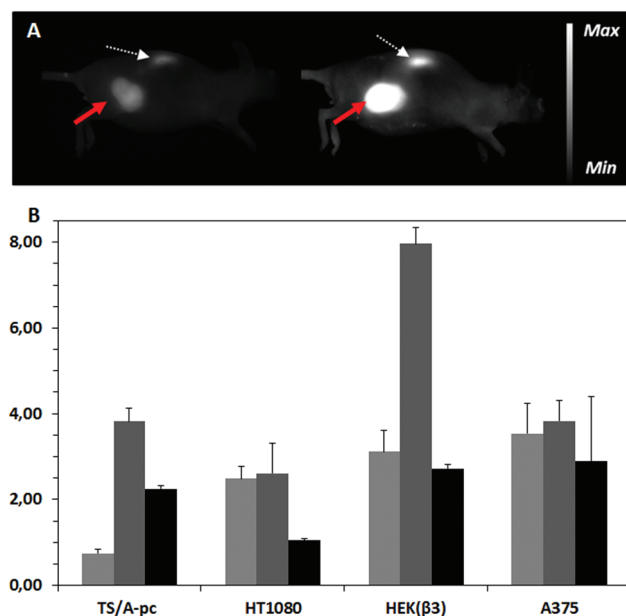


Fig. 4 (A) Fluorescence images of subcutaneous HEK(β_3) tumor-bearing Swiss nude mice at 5 hours after intravenous injection of 2 nmol compound **1** (right) compared to 2 nmol compound **7** (left) (red arrow: tumor; white arrow: kidney; exposition time: 500 ms). (B) Tumor to muscle ratio of nude mice bearing tumor at 24 h after intravenous injection of 2 nmol MMPsense 680 (light grey bar), 2 nmol activatable fluorescent **1** (dark grey bar), or 2 nmol control Cy5-containing peptide **7** (dark bar).

introducing an MMP peptidic sequence for tumor detection as the dequenching from the MMP protease increases the tumor to muscle ratio.

Conclusion

In summary, a dual-specific MMP-activatable RGD compound was synthesized *via* iterative oxime ligations of peptide fragments. The ensuing compound was then evaluated through *in vitro* and *in vivo* experiments. Having established the principle of protease-activatable RGD targeting *in vivo*, we provide a strong molecular rationale for improving the design of targeted drug delivery vectors. An extension of the system combining a cytotoxic peptide and the MMP-activatable RGD compound is in progress and will be reported in due course.

Experimental section

RGD-containing peptide 5

Linear decapeptide was assembled on 2-chlorotriethylchloride resin using building blocks and the subsequent head-to-tail cyclization was carried out as previously described affording peptide **4** that was used in the next step without further purification (see the ESI†).¹⁴

Full deprotection of peptide **4** (157.2 mg, 86 μ mol) was carried out using 10 mL of a solution containing TFA-H₂O-TIS (95 : 2.5 : 2.5) at room temperature for 3 h. The product was

isolated after removal of solvents under reduced pressure and precipitation from diethyl ether to yield deprotected peptide as a white powder in quantitative yield (169 mg, 86 μmol). In parallel, cyclo[-Arg-Gly-Asp-D-Phe-Lys(-CO-CHO)-] was synthesized as previously described.²⁰

To an aqueous solution (2 mL) containing the deprotected peptide (20 mg, 10.2 μmol) was added freshly prepared cyclo [-Arg-Gly-Asp-D-Phe-Lys(-CO-CHO)-] (67.5 mg, 87 μmol). The reaction mixture was stirred for 1 h at 25 °C. The RGD-containing conjugate was isolated after purification by RP-HPLC as a white powder (40.1 mg, 8.8 μmol , 86%). A serine oxidation of an RGD-containing conjugate (20 mg, 4.3 μmol) by an aqueous solution containing 10 equiv. of NaIO₄ (10.8 mg, 50.4 μmol) afforded the aldehyde component **5**. The product was directly purified by RP-HPLC to yield compound **5** as a white powder (14.6 mg, 3.3 μmol , 77%).

MMP peptide 6

Peptide synthesis was carried out as described in the general procedure (see the ESI[†]). Full deprotection of protected peptide (Boc)₂NO-CH₂-CO-Gly-Lys(Boc)-Gly-Pro-Gln(Trt)-Gly-Leu-Ala-Gly-Gln(Trt)-Lys(Boc)-Gly-OH (20 mg, 9.8 μmol) was done from a solution of TFA-H₂O-TIS-EDT (90 : 5 : 2.5 : 2.5) for 2 h. The product was directly purified by RP-HPLC to yield compound **6** as a white powder (6 mg, 4 μmol , 41%).

Fluorescent conjugate 1

To a solution containing the derivative **5** (17 mg, 3.8 μmol) in 400 μL of H₂O-CH₃CN (1 : 1) was added the peptide **6** (6 mg, 4 μmol). The reaction mixture was stirred for 3 h at 25 °C. An MMP-containing conjugate was isolated after purification by RP-HPLC as a white powder (10 mg, 1.7 μmol , 46%). To a solution containing the MMP-containing conjugate (4 mg, 0.7 μmol) in 180 μL of DMF was added 3 μL DIPEA and cyanine 5-mono NHS ester (1.7 mg, 1.8 μmol). The reaction mixture was stirred overnight at room temperature. The product was directly purified by RP-HPLC to yield compound **1** as a blue powder (1.5 mg, 0.22 μmol , 31%).

Fluorescence analysis

Experiments were carried out by using 200 μL of 0.25 μM of compound **1** or control Cy-5 containing peptide in 50 mM Tris buffer (pH 7.5) with 150 mM NaCl, 5 mM CaCl₂ and 0.05% Brij-35 at 37 °C. Spectra were recorded from 650 to 750 nm. Samples were incubated at 37 °C and their spectra measured before incubation with the enzyme matrix metalloproteinase-9. Then, samples were incubated with 5 nM of MMP-9 at 37 °C for 24 hours (see also the ESI[†]).

In vivo fluorescence imaging

Nude mice (6–8 weeks old) received a sub-cutaneous xenograft of HEK293(β 3) cells (20 \times 10⁶ per mouse), HT1080 (10 \times 10⁶ per mouse), A375 (10 \times 10⁶ per mouse), or TS/A-pc cells (5 \times 10⁶ per mouse). After tumor growth, mice ($n = 3$ for each group) were anesthetized (isoflurane/oxygen 4%/3.5% for induction and 2% thereafter) and were injected intravenously

into the tail vein with 200 μL of compound **1** or Cy5 control peptide (2 nmol) or 150 μL of MMPsense 680 (2 nmol), then they are illuminated by 633 nm (cyanine 5 compounds) or 660 nm (MMPsense) light-emitting diodes equipped with interference filters. Fluorescence images are acquired by a back-thinned CCD camera at -80 °C. After imaging at different time points after injection (30 minutes, 1 hour, 2 hours, 3 hours, 5 hours and 24 hours), the mice were sacrificed (at either 3 hours or 24 hours after injection) and dissected for imaging organs (see also the ESI[†]).

Acknowledgements

This work was supported by the Institut National du Cancer (INCA), the Université Joseph Fourier, the Centre National de la Recherche Scientifique (CNRS), and the NanoBio program for the facilities of the Synthesis platform.

Notes and references

- 1 J. S. Desgrosellier and D. A. Cheresch, *Nat. Rev. Cancer*, 2010, **10**, 9.
- 2 (a) M. Pfaff, K. Tangemann, B. Müller, M. Gurrath, G. Müller, H. Kessler, R. Timpl and J. Engel, *J. Biol. Chem.*, 1994, **269**, 20233; (b) W. Arap, R. Pasqualini and E. Ruoslahti, *Science*, 1998, **279**, 377.
- 3 (a) K. Temming, R. M. Schiffelers, G. Molema and R. J. Kok, *Drug Resist. Updates*, 2005, **8**, 381; (b) E. Garanger, D. Boturyn and P. Dumy, *Anti-Cancer Agents Med. Chem.*, 2007, **7**, 552.
- 4 R. Haubner, W. A. Weber, A. J. Beer, E. Vabuliene, D. Reim, M. Sarbia, K.-F. Becker, M. Goebel, R. Hein, H.-J. Wester, H. Kessler and M. Schwaiger, *PLoS Med.*, 2005, **2**, e70.
- 5 W. Cai, D.-W. Shin, K. Chen, O. Gheysens, Q. Cao, S. X. Wang, S. S. Gambhir and X. Chen, *Nano Lett.*, 2006, **6**, 669.
- 6 M. Keramidis, V. Josserand, C. A. Righini, C. Wenk, C. Faure and J. L. Coll, *Br. J. Surg.*, 2010, **97**, 737.
- 7 S. Foillard, Z. Jin, E. Garanger, D. Boturyn, M.-C. Favrot, J.-L. Coll and P. Dumy, *ChemBioChem*, 2008, **9**, 2326.
- 8 S. Foillard, L. Sancey, J.-L. Coll, D. Boturyn and P. Dumy, *Org. Biomol. Chem.*, 2009, **7**, 221.
- 9 E. S. Olson, T. Jiang, T. A. Aguilera, Q. T. Nguyen, L. G. Ellies, M. Scadeng and R. Y. Tsien, *Proc. Natl. Acad. Sci. U. S. A.*, 2010, **107**, 4311.
- 10 G. Bergers, R. A. Brekken, G. McMahon, T. H. Vu, T. Itoh, K. Tamaki, K. Tanzawa, P. Thorpe, S. Itohara, Z. Werb and D. Hanahan, *Nat. Cell Biol.*, 2000, **2**, 737.
- 11 N. Ramos-DeSimone, E. Hahn-Dantona, J. Siple, H. Nagase, D. L. French and J. P. Quigley, *J. Biol. Chem.*, 1999, **274**, 13066.
- 12 J. Razkin, V. Josserand, D. Boturyn, Z. Jin, P. Dumy, M. Favrot, J.-L. Coll and I. Texier, *ChemMedChem*, 2006, **1**, 1069.
- 13 E. Garanger, D. Boturyn, O. Renaudet, E. Defrancq and P. Dumy, *J. Org. Chem.*, 2006, **71**, 2402.

- 14 S. Foillard, M. Olsten Rasmussen, J. Razkin, D. Boturny and P. Dumy, *J. Org. Chem.*, 2008, **73**, 983.
- 15 Φ/Φ (Cy5): relative fluorescence quantum yield of **1** in PBS (excitation at 649 nm, emission at 665 nm).
- 16 E. Garanger, D. Boturny, Z. Jin, P. Dumy, M.-C. Favrot and J.-L. Coll, *Mol. Ther.*, 2005, **12**, 1168.
- 17 B. M. Wallis de Vries, J.-L. Hillebrands, G. M. van Dam, R. A. Tio, J. S. de Jong, R. H. J. A. Slart and C. J. Zeebregts, *Circulation*, 2009, **119**, e534.
- 18 Z. Jin, V. Josserand, J. Razkin, E. Garanger, D. Boturny, M.-C. Favrot, P. Dumy and J.-L. Coll, *Mol. Imaging*, 2006, **5**, 188.
- 19 A. Faust, B. Waschkau, J. Waldeck, C. Höltke, H.-J. Breyholz, S. Wagner, K. Kopka, W. Heindel, M. Schäfers and C. Bremer, *Bioconjugate Chem.*, 2008, **19**, 1001.
- 20 D. Boturny and P. Dumy, *Tetrahedron Lett.*, 2001, **42**, 2787.